ANTIBACTERIAL ACTIVITY AND FLUORESCENCE PROPERTIES OF 4,7-DICHLORO-2-QUINOLINEMETHYLACRYLATE

HERNÁN VALLE [a,*], RAMALINGA VISWANATHAN MANGALARAJA [a,b,*], LUIS AGUILAR [c,d],
CARLOS CARRASCO [c], NATALIA PADILLA [c], MOHAMED DAHROUCH [e], BERNABÉ RIVAS [f],
AND HOMERO URRUTI A [c,g]

[a]*Advanced Ceramics and Nanotechnology Laboratory, Department of Materials Engineering, Faculty of Engineering, University of Concepción, Concepción 4070409, Chile*
[b]*Technological Development Unit (UDT), University of Concepción, Coronel Industrial Park, Coronel, Chile*
[c]*Biofilm and Environmental Microbiology Laboratory, Biotechnology Center, University of Concepción, P.O. Box 160-C, Concepción, Chile*
[d]*Environmental Science Faculty and Center EULA-Chile, University of Concepción, P.O. Box 160-C, Concepción, Chile*
[e]*Department of Organic Chemistry, Faculty of Chemical Sciences, University of Concepción, P.O. Box 160-C, Concepción, Chile*
[f]*Polymer Department, Faculty of Chemical Sciences, University of Concepción, Concepción 4089100, Chile*
[g]*Department of Microbiology, Faculty of Biological Sciences, University of Concepción, P.O. Box 160-C, Concepción, Chile*

ABSTRACT

Currently, some quinoline-based anticancer drugs are successful repurposed for treatment of bacterial infections. This study assessed the antibacterial activity of the new anticancer compound 4,7-dichloro-2-quinolinemethylacrylate (AQM) against bacteria of both clinical and agricultural interest, and also determined the influence of some metal cations (Fe^{3+}, Mn^{2+}, Zn^{2+}, Na^+, Mg^{2+}, Co^{2+} and Ni^{2+}) on the AQM photophysics. The synthesis of AQM was carried out by the reported method. The antibacterial activity of AQM on *Pectobacterium carotovorum subsp. carotovorum (Pcc)*, *Ralstonia solanacearum*, *Klebsiella pneuminiae*, *Pseudomonas syringae*, *Staphylococcus aureus* y *Bacillus sp.*, was evaluated using the spectrophotometric method of broth microdilution. At 125 ppm, AQM produced growth inhibition of 51.7% in *Pcc*, and a bacteriostatic effect in *S. aureus* and *Bacillus sp.*, but no effect was seen against the other bacteria. In addition, fluorescence quenching of AQM solution induced only by Fe^{3+} ion, and not by the other metal cations, was confirmed. These results postulate that AQM could be a molecule with potential application in antibacterial therapy or in the fluorometric detection of Fe^{3+} ions.

Keywords: Quinoline, antibacterial activity, fluorescence quenching, broth microdilution.

1. INTRODUCTION

A large number of quinoline-like molecules are known to have biological activities of pharmacological interest, such as: antimalarial, antiprotozoal, antifungal, anthelmintic, antiviral, antialzheimer, antipsychotic, antiasmatic, antiglaucoma, cardiotonic, anesthetic, anticancer, and especially, antibacterial.[1–4] The FDA has aproved 4-quinolones-like molecules (norfloxacin, ciprofloxacin and levofloxacine)[5] and 8-hydroxyquinolines-like molecules (clioquinol and nitroxoline)[6,7] for use in pharmaceutical trials in humans. The mechanisms of action of 4-quinolones and 8-hydroxyquinolines against bacteria have been previously reported. The 4-quinolones inhibit the topoisomerase enzyme, whose main function is to unwind the double strand of bacterial DNA allowing the ribosome to advance during the genome replication and, therefore, the interruption of this process causes the bacterial death.[5,8–10] For the 8-hydroxyquinolines, some research suggest that the antibacterial effect of these molecules is due to their high chelating capacity of divalent cations (Mg^{2+}, Mn^{2+}, Ca^{2+}) that allow them to bind to metal cofactors of bacterial enzymes and, consequently, inhibit the enzymatic activity.[7,11] Other types of quinoline-like molecules with antibacterial activity, which contain various functional chemical groups, are discovered year after year, but not all of them are submitted to the FDA for pre-clinical studies.[3,12–14]

Several studies have reported that some quinoline-like molecules with antibacterial activity can be used as new anticancer agents, either by administering them individually or in combination with another conventional anticancer drug. Some examples of the latter are: nitroxoline,[15–18] clioquinol,[19,20] iodoquinol, oxyquinoline,[21] bedaquiline,[22,23] ciprofloxacin and levofloxacin.[23] On the other hand, there are also some reports of quinoline-based anticancer drugs used successfully as treatment for bacterial infections (e.g., camptothecin derivatives).[24] This double biological activity is probably due to the similarity of certain biochemical processes of human and bacterial cells (e.g., cell division or cellular respiration) in which structurally similar biomolecules participate, which would be the therapeutic target for these quinolinic drugs.[8]

It is noteworthy that Valle et al. recently reported the synthesis of the new molecule AQM, which showed potent cytotoxic activity against breast carcinoma cells MDA-MB-453 (IC_{50}: 19 μM);[25] however, its potential antibacterial activity has not been evaluated. In the present work, we investigated the antibacterial activity of AQM on six bacterial species, two pathogenic bacteria for humans (*Klebsiella pneuminiae* and *Staphylococcus aureus*), three phytopathogenic bacteria (*Pcc*, *Ralstonia solanacearum* and *Pseudomonas syringae*) and *Bacillus sp*. In addition, some fluorescence properties of AQM were examined in tetrahydrofuran.

2. EXPERIMENTAL SECTION

2.1. Reagents and Materials

To AQM's synthesis the following reagents were used without further purification: 3-chloroaniline, ethyl acetoacetate, phosphorus oxychloride ($POCl_3$), benzoyl chloride (Bz-Cl), acryloyl chloride, triethylamine (TEA), diphenyl ether, n-hexane, ethanol, methanol, diethyl ether, dichloromethane (DCM), ethyl acetate (AcOEt), tetrahydrofuran (THF), sodium hydroxide (NaOH), hydrochloric acid (HCl, 37% v/v), sodium bicarbonate ($NaHCO_3$), sodium sulfate anhydrous (Na_2SO_4) and 3-chloroperbenzoic acid (3-CPBA, 72% w/w). The analytical grade nitrate salts: $Zn(NO_3)_2 \cdot 6H_2O$, $Ni(NO_3)_2 \cdot 6H_2O$, $Mg(NO_3)_2 \cdot 6H_2O$, $Co(NO_3)_2 \cdot 6H_2O$, $Mn(NO_3)_2 \cdot xH_2O$, $Fe(NO_3)_3 \cdot 9H_2O$ and $NaNO_3$, were employed as sources of metal cations for the fluorescence quenching measurements. All reagents were supplied by Merck, except 3-CPBA and nitrate salts, which were provided by Acros Organic and Sigma-Aldrich, respectively. Double-distilled water (DDW) was used throughout all experiments.

Merck silica gel 60 F_{254}-coated aluminium plates (10×5 cm), n-hexane-ethyl acetate (1:1), and an ultraviolet lamp (CAMAG, 254 and 366 nm) were used to assess the purity of the compounds by thin layer chromatography (TLC). Flash column chromatography was conducted over Merck silica gel 60 (0.063-0.200 mm / 70-230 mesh ASTM).

2.2. Synthesis of 4,7-dichloroquinaldine

In a 2000-mL round bottom flask 418.6 mL of 3-chloroaniline (4 mol), 510.6 mL of ethyl acetoacetate (4 mol), 2 mL of HCl (37% v/v) and 166 g of anhydrous Na_2SO_4, were mixed in that order. Then the container was sealed and maintained under magnetic stirring for 72 hours at 25 °C. Subsequently, the insoluble Na_2SO_4 was separated by decantation and the supernatant was filtered under vacuum using filter paper (Whatman N°2). 812 mL of a translucent yellow oily liquid were obtained (crude ethyl β-(3-chloroanilino)crotonate).

In other 2000-mL round bottom flask equipped with condenser, dropping funnel and thermometer, 1000 mL of diphenyl ether were heated to 250 °C under stirring, using a heating mantle with built-in magnetic stirrer. 200 mL of the yellow oil of the first step (crude ethyl β-(3-chloroanilino)crotonate), contained in the dropping funnel, were added dropwise into the hot diphenyl ether (250 °C) over a period of 0.5 h and both heating and stirring were continued for an additional 10 h. After this time the reaction mixture was allowed to cool to 60 °C and the solid formed was filtered under vacuum, washed with abundant n-hexane until all residual diphenyl ether was removed, and thoroughly dried in the oven at 60 °C. 45 g of a beige powder was obtained (crude 7-chloro-4-hydroxyquinaldine).

Subsequently, in a 250-mL round bottom flask equipped with a condenser, a mixture of 90 mL of POCl₃ and 45 g of crude 7-chloro-4-hydroxyquinaldine was heated at 100 °C under constant stirring. The reaction mixture was cooled to room temperature, slowly poured into ice-water (500 mL) and basified with 4 M NaOH to pH 8. The solid produced was triturated, washed with water, filtered under vacuum and dried at 60 °C; It was then dissolved in DCM and purified by flash chromatography on silica gel 60 (0.063-0.200 mm) using DCM as eluent. The elute was concentrated in vacuo to give a white-yellowish solid (28 g), which was recrystallized from ethanol-water to obtain 25.5 g of white needle-shaped crystals, identified by ¹H NMR spectroscopy as 4,7-dichloroquinaldine.

2.3. Synthesis of 4,7-dichloro-2-quinolinemethylbenzoate (2QMB)

To a solution of 4,7-dichloro-quinaldine (25.03 g, 118 mmol) in dichloromethane (200 mL) was added 3-CPBA (24.85 g, 144 mmol). The reaction mixture was heated at 60°C for 6 h under magnetic stirring and then washed with saturated aqueous NaHCO₃ (400 mL). The dichloromethane layer was dried over Na₂SO₄ and the solvent evaporated in vacuo to give 4,7-dichloroquinaldine-N-oxide (NOQ) as a yellowish white powder, which was used without further purification. To a solution of NOQ (25 g, 110 mmol) in dichloromethane (300 mL) was added benzoyl chloride (15 mL, 129 mmol), mixed, and then heated at 60°C under nitrogen atmosphere for 18 h. After this period, the reaction mixture was cooled to room temperature and washed with 1 M NaOH aqueous solution (2×300 mL), followed by brine washing (300 mL), Na₂SO₄ drying, and concentration under vacuum to obtain a solid residue (2QMB), which was recrystallized from hot methanol.

2.4. Synthesis of 4,7-dichloro-2-quinolinemethanol (QM)

To a solution of 2QMB (17 g, 50 mmol) in 82% v/v acetone aqueous (1000 mL) was added a solution of NaOH (4 g, 100 mmol) in water (20.4 mL). The reaction mixture was stirred at 35°C for 1 h, before further water was added (500 mL). The pH of the mixture was adjusted to ~7 with 6 M HCl. The mixture was concentrated to half the volume under vacuum, and subsequently extracted with DCM (2×200 mL). The combined organic layers were washed with brine, dried over Na₂SO₄, and concentrated by vacuum distillation to obtain a solid (QM), which was washed with diethyl ether.

2.5. Synthesis of 4,7-dichloro-quinolinemethyl acrylate (AQM)

QM (9 g, 40 mmol) and triethylamine (33.3 mL, 240 mmol) dissolved in 900 mL of anhydrous THF were placed in a round-bottomed, three-necked flask equipped with a dropping funnel. Then 9.7 mL of acryloyl chloride (120 mmol) diluted with 57 mL of THF were added dropwise into the mixture, under nitrogen atmosphere and with stirring at 10°C. The reaction was allowed to proceed at room temperature for 3 h, and the reaction mixture was then partitioned between 5% w/v NaHCO₃ aqueous (500 mL) and AcOEt (500 mL). The aqueous phase was re-extracted with AcOEt (500 mL) and the combined organic phases washed with water (500 mL), dried over Na₂SO₄ and concentrated until dryness under vacuum distillation to give the solid product, AQM.

2.6. Spectroscopic characterization

A NMR Bruker Ascend™ 400 MHz spectrometer, chloroform-*d* (CDCl₃, 98%, Sigma-Aldrich) or dimethyl sulfoxide-*d₆* (DMSO-*d₆*, 99.96%, MagniSolve™) and NMR sample tubes were used to elucidate the structure of compounds (obtained from each synthesis step of AQM) by proton NMR (400 MHz) and/or carbon-13 NMR (100 MHz) techniques. Each synthetized compound was dissolved in deuterated solvent at a concentration of 30 mg mL⁻¹. UV absorption spectrum of AQM in THF solution was recorded at room temperature using a

Shimadzu UV-2600 spectrophotometer (with quartz cuvette of 1×1 cm and 0.2 nm absorbance slit width), which was controlled by Shimadzu UVProbe software.

2.7. Fluorescence quenching measurements

The fluorescence quenching ability of different metal ions (Zn²⁺, Ni²⁺, Mg²⁺, Co²⁺, Mn²⁺, Fe³⁺ and Na⁺) onto the AQM solution was investigated. Firstly, all the metal ions were dissolved in water (DDW) at 100 mM concentration. Then 45.4 µL of metal ion solution was added into a 5 mL of 2.42 mM AQM solution (in THF) at ambient temperature, resulting a metal ion concentration about 0.9 mM in the AQM solution. The metal ions able to quench inherent fluorescence from AQM solution were studied as quenchers at various concentrations (0.05–0.9 mM) by fluorescence spectroscopy. The fluorescence spectra of AQM and their respective AQM-metal ion complex (in THF solution) were measured on a Photon Technology International (PTI) Quantamaster fluorometer (with quartz cuvette of 1×1 cm and 5 nm excitation and emission slit widths), which was controlled by PTI FelixGX software (version 4.0.2).

2.8. Antibacterial Assay

The six bacterial isolates, two pathogenic bacteria for humans (*Klebsiella pneumoniae* and *Staphylococcus aureus*), three phytopathogenic bacteria (*Pcc*, *Ralstonia solanacearum* and *Pseudomonas syringae*) and *Bacillus sp.*, were supplied from the Biofilm and Environmental Microbiology Laboratory (Center of Biotechnology) of University of Concepción. All the bacterial were maintain routinely on Tripticase Soy Broth (TBS).

A modified broth microdilution method based on the National Committee for Clinical Laboratory Standards guidelines[26] was used to assess the antibacterial activity of AQM against the bacterial strains. AQM stock solution of 2500 ppm was prepared using 10% DMSO-TSB as solvent, and further ten-fold serial diluted in 5 steps using TSB to produce dilutions of 1:10¹ to 1:10⁵. From an overnight culture, a bacterial suspension was adjusted to a concentration of ~1×10⁸ CFU mL⁻¹ (0.5 McFarland standard), and then diluted to 1:10² into TSB. Briefly, 80 µL of TSB was added into wells of a 96-well microtiter plate. To these, 100 µL of each AQM ten-fold serial dilutions was separately added, followed by the addition of 20 µL of the bacterial suspension. Thus, the AQM final concentrations were: 125, 12.5, 1.25, 0.125 and 0.0125 ppm, while the bacterial final concentration was about 1×10⁵ CFU mL⁻¹ in each well. To test if DMSO has an antibacterial activity, solutions containing DMSO dissolved in TSB at 0.5, 0.05, 0.005, 0.0005, and 0.00005% were prepared to use as control. Afterward, the growth of bacteria at 37°C was measured in terms of optical density at 600 nm (OD600), during ~20 h at 1-hour intervals, using an automated plate reader TECAN Infinite Pro 2000. A mild and discontinuous agitation for 10 s before the measurement was carried out. The antibacterial rate (AR) was calculated according the following equation:

$$AR\ (\%) = \frac{(OD\ test - OD\ blank)}{OD\ control}\ x\ 100$$

Where "OD *test*" is OD600 value from the well with AQM plus bacteria plus culture medium; "OD *blank*" is OD600 value from the well with AQM plus culture medium (without bacteria); and "OD *control*" is OD600 value from the well with bacteria plus culture medium.

To assess the bactericidal activity of AQM, sub-cultures were prepared by transferring 100 µL from the wells with treatment to 5 mL of culture medium without AQM and allowed to grow for 24 h, verifying the growth of bacteria by presence or absence of turbidity. All experiments were carried out in triplicate.

3. RESULTS AND DISCUSSION

3.1. Synthesis of AQM

The synthesis procedure for obtaining AQM and some of its precursors, such as 4,7-dichloroquinaldine, 2QMB and QM, is shown in Scheme 1. Step [a] for the synthesis of 4,7-dichloroquinaldine (59% yield) involved three reactions: an acid-catalyzed condensation of 3-chloroaniline with ethyl acetoacetate to form ethyl β-(3-chloroanilino)crotonate, followed by its thermal cyclization in diphenyl ether under reflux conditions (Conrad-Limpach method), and subsequent chlorination of the intermediate 7-chloro-4-hydroxyquinaldine with

POCl₃.[27] In step [b], 4,7-dichloroquinaldine is first converted into its corresponding N-oxide by reaction with 3-CPBA (92 % yield), and then is transformed into its N-benzoyloxy derivative by consecutive reaction with Bz-Cl, followed by rearrangement of the benzoyloxy group from N-1 to the C-2 methyl group to form 2QMB ester (48% yield).[28]
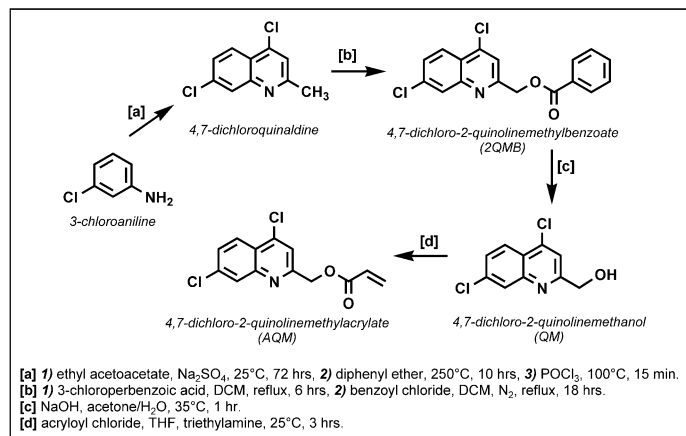
Scheme 1. Synthesis of AQM.

In step [c] 2QMB ester underwent basic hydrolysis to produce the QM alcohol (60% yield). Finally, in step [d], the esterification of QM with acryloyl chloride is performed to produce AQM (95% yield). The overall yield of the AQM synthesis (calculated based on 3-chloroaniline) was 15%. Its ¹H NMR spectrum in DMSO-d_6 (Figure 1) shows four aromatic proton signals designated as *a*, *b*, *c* and *d*, which are located in the region between δH 8.20-7.70. The *doublet* signal at δH 8.16 with *ortho*-coupling of 9.0 Hz is attributed to *b*, and the *doublet* signal at δH 8.07 with *meta*-coupling of 2.1Hz is assignated to *d*. Meanwhile, *c* corresponds to the *double-doublet* signal at δH 7.75 with *ortho*- and *meta*-coupling of 9.0 and 2.1 Hz respectively, confirming the position of one chlorine atom at C-7. The *singlet* signal appearing at δH 7.80 is attributed to *a*. A second region of signals between δH 6.00 and 6.50 belongs to the three vinyl protons designated as *f*, *g* and *h*. The *h* signal corresponds to the *double-doublet* centred at δH 6.45 with *trans*- and *geminal*-coupling of 17.3 Hz and 1.6 Hz ($^3J_{hf}$ and $^2J_{hg}$) respectively.

The signal for *f* at δH 6.33 is also a *double-doublet*, but with *trans*- and *cis*-coupling of 17.3 Hz and 10.2 Hz ($^3J_{hf}$ and $^3J_{gf}$); and the signal for *g* at δH 6.04 is again a *double-doublet*, this time with *geminal*- and *cis*-coupling of 1.6 Hz and 10.2 Hz ($^2J_{hg}$ and $^3J_{gf}$) respectively. Finally, the singlet at δH 5.40 is attributed to the two *e* protons of the methylene group that connects both the quinoline ring and acrylic moiety.
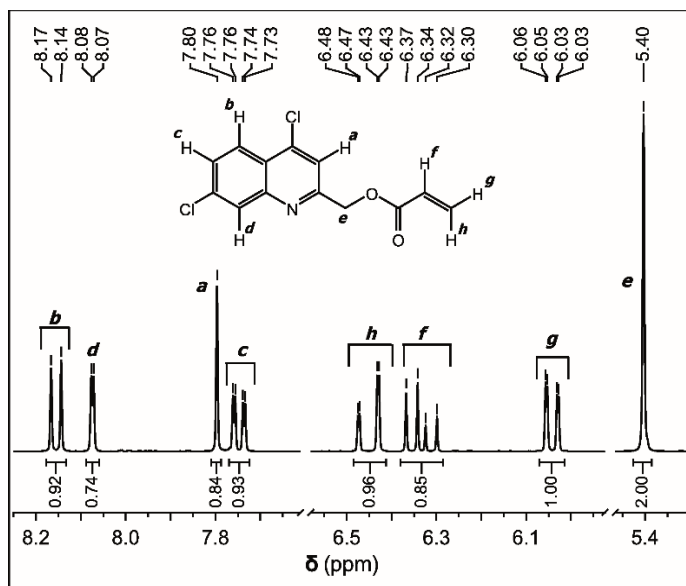

Figure 1. ¹H NMR spectrum of AQM in DMSO-d₆.

Additionally, ¹³C NMR spectrum of AQM (Figure S1, supporting information) shows signals for: (1) six quaternary carbons of which five are aromatics (C-2, C-4, C-7, C-9 and C-10, between δ 120 and 160) and one is from a ester carbonyl group (C-11, at δ 165.11), (2) four aromatic methine carbons (C-3, C-5, C-6 and C-8, between δ 119 and 128), (3) two olefinic carbons (C-12 and C-13, between δ 128 and 133), and (4) one methylene carbon (C-1, at δ 65.99). Both the ¹H NMR and ¹³C NMR (in DMSO-d_6) spectra of AQM show all of the signals matching with the expected structure. On the other hand, structural elucidation of compounds 4,7-dichloroquinaldine, 2QMB and QM was performed based on the analysis of ¹H NMR spectra shown in Figures S2-S4 (in supporting information) and by comparing of these spectral data with those reported in literature. AQM and 2QMB are new molecules, however, 4,7-dichloroquinaldine and QM have been reported by Singh et al.[27] and Esparza-Ruiz et al.[29] respectively.

3.2. Photophysics properties of AQM in THF solution

The fluorescence emission and UV–visible absorption spectra of AQM in THF solution are shown in Figure 2. The UV-visible spectrum exhibited a pronounced absorption maximum peak at 324 nm that corresponds to the π–π* transition of quinoline group. In the fluorescence spectrum, the emission maximum was observed around 409 nm when excited at 324 nm. The difference between the absorption ($λ_A$ = 324 nm) and emission ($λ_F$ = 409 nm) maximum wavelengths (expressed in wavenumbers, cm⁻¹) is known as Stokes shift, an important parameter which provides information about structure and properties between the ground S_0 state and the first excited S_1 state of the fluorophores.[30] The calculated value of Stokes shift for AQM is 6320 cm⁻¹, a relatively large value which could be attributed to the change in the electron density of the compound upon excitation. The fluorescence quantum yield ($Φ_F$) is the ratio of the number of emitted photons to the number of absorbed photons by the fluorophore molecules, and is calculated using the following equation:

$$Φ_F^x = Φ_F^r \frac{S_x}{S_r} \frac{A_r}{A_x} \frac{n_x^2}{n_r^2}$$

Where the designators x and r indicate sample and reference, respectively, $Φ_F$ is the fluorescence quantum yield, A is the absorbance intensity, S is the integrated emission area and n is the solvent refractive index. The $Φ_F$ value of AQM in THF, calculated by above equation, is 0.101 by using pyrene in THF ($Φ_F$ = 0.79) as standard reference.[31]
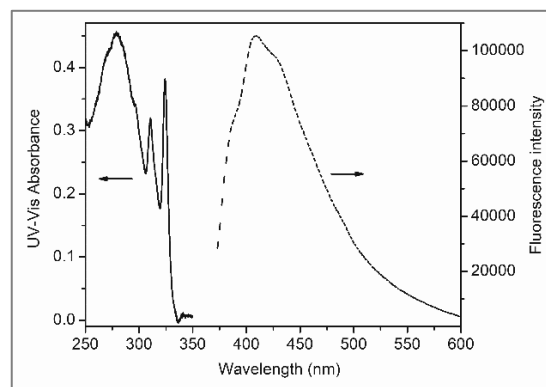
**Figure 2.** Normalized absorption and fluorescence emission spectra of AQM in THF at a concentration of 100 μM.

3.2. Influence of metal cations on the AQM photophysics

The metal cations Fe^{3+}, Mn^{2+}, Zn^{2+}, Na^+, Mg^{2+}, Co^{2+} and Ni^{2+} are essential for bacterial growth. The effect of these metal cations on the fluorescence emission of AQM in THF solution, was determined by measuring of the values of relative fluorescence intensity (I/I_0), defined as the ratio between fluorescence intensities (at maximum emission peak, $λ_F$ = 409 nm) after and before addition of metal cations to the AQM solution. As shown in Figure 3, the relative fluorescence intensity (I/I_0) suddenly decreased with the addition of Fe^{3+}, while the other tested cations (0.9 mM) did not markedly change the relative fluorescence intensity, thus it can be concluded that this system is selective for Fe^{3+}.
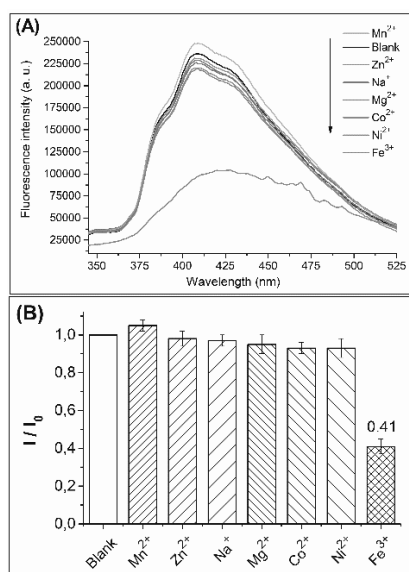
Figure 3. Fluorescence quenching of AQM in THF solution by the addition of different metal cations dissolved in water (λ_{ex}= 324 nm, the concentrations of AQM and metal cation are 2.4 mM and 0.9 mM, respectively). Each experiment was done in duplicate.

Figure 4A shows the fluorescence spectrum intensity of AQM solution decreasing as Fe^{3+} concentration increases. Moreover in Figure 4B, a linear relationship between the fluorescence quenching (I_0/I) and the Fe^{3+} concentration is observed between 0.05 and 0.9 mM, which is consistent with the Stern–Volmer equation[30] and, therefore, suitable for the quantification of Fe^{3+} in this range of concentrations. From the Stern–Volmer equation, $I_0/I = 1 + K_{sv}[Q]$, the K_{sv} constant was calculated, which represents the efficiency of the fluorescence quenching. The others terms in the equation are the quencher concentration, [Q], and the maximum fluorescence intensities of the AQM solution in the absence and presence of Fe^{3+} (quencher), I_0 and I, respectively. The K_{sv} value obtained of AQM for Fe^{3+} was 1.62×10^3 M^{-1}, indicating that this compound has a moderate sensitivity for Fe^{3+} ion in comparison to others compounds such as julolidine derivatives (3.3×10^4 M^{-1})[32] and rhodamine derivatives (2.46×10^4 M^{-1}).[33] This result is indicative of a possible iron (III) chelating activity of AQM which leads to a significant fluorescence quenching of the AQM solution.[34,35]
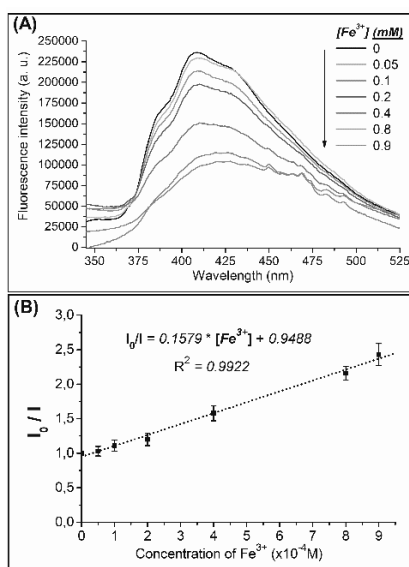

Figure 4. (A) Fluorescence emission spectra of AQM in THF solution at various concentrations of Fe^{3+} cation (λ_{ex}= 324 nm). (B) Linear relationship between the relative fluorescence quenching of AQM and the Fe^{3+} concentration. The AQM concentration was held at 2.4 mM. Each point in (B) represent the mean ± standard deviation (SD) of three independent experiments.

3.3. Antibacterial Assay

The cultures of *Ralstonia solanacearum, Klebsiella pneuminiae* and *Pseudomonas syringae* treated with AQM at a concentration of 125 ppm (Figures 5-7) produced OD600 values similar to those of the respective culture without treatment (blank – DMSO) within the time range tested, indicating absence of antibacterial effect. On the other hand, the cultures of *Staphylococcus aureus* and *Bacillus sp*. treated with AQM at the same concentration (Figures 8 and 9) produced near-zero and constant OD600 values during the 20 hours of treatment, which demonstrates the antibacterial effect of AQM on these Gram-positive bacteria. The bactericidal assay showed that AQM has not bactericidal effect on the bacterial strains in the range of tested concentrations, this indicating a bacteriostatic effect of this molecule. As regards Pcc bacteria subjected to the same treatment (AQM at 125 ppm), the OD600 values trend in Figure 10 showed a reduction in the growth rate during the first 14 hours (probably associated with a prolonged Lag phase), followed by a stationary phase until the end of experiment.
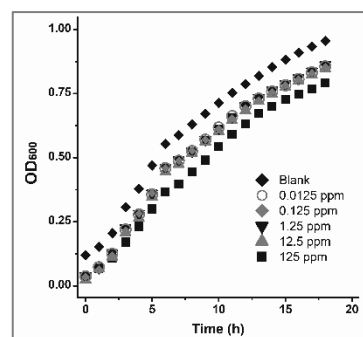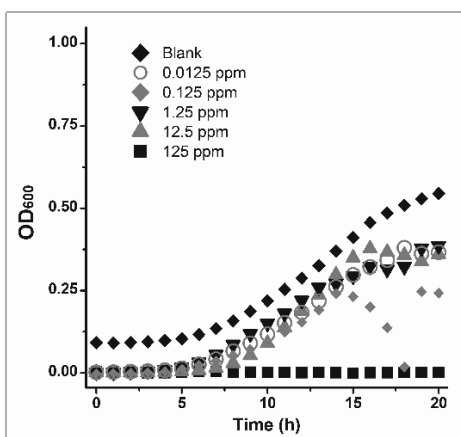

Figure 5. Antimicrobial effect of the AQM molecule on *R. solanacearum*. OD600 is optical density at 600 nm. Each point presents the mean of three measurements. The SD bars were deleted for clarity.
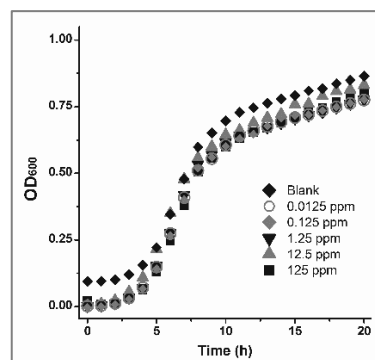
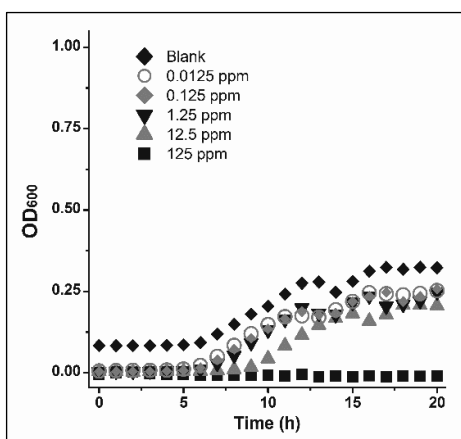**Figure 6.** Antimicrobial effect of the AQM molecule on *K. pneumoniae*. OD600 is optical density at 600 nm. Each point presents the mean of three measurements. The SD bars were deleted for clarity.
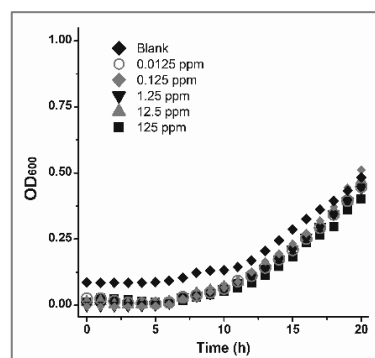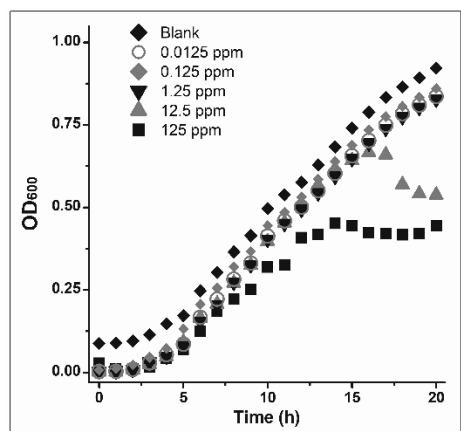

Figure 7. Antimicrobial effect of the AQM molecule on *P. syringae*. OD600 is optical density at 600 nm. Each point presents the mean of three measurements. The SD bars were deleted for clarity.

Figure 8. Antimicrobial effect of the AQM molecule on *S. aureus*. OD600 is optical density at 600 nm. Each point presents the mean of three measurements. The SD bars were deleted for clarity.

Figure 9. Antimicrobial effect of the AQM molecule on *Bacillus sp*. OD600 is optical density at 600 nm. Each point presents the mean of three measurements. The SD bars were deleted for clarity.

Figure 10. Antimicrobial effect of the AQM molecule on *Pectobacterium carotovorum subsp. Carotovorum, Pcc*. OD600 is optical density at 600 nm. Each point presents the mean of three measurements. The SD bars were deleted for clarity.

The antibacterial rates (%) of AQM against these bacteria are shown in Table 1. The DMSO concentrations tested shows no bacteriostatic or bactericidal effect against the bacterial strains. The antibacterial effect of AQM against *S. aureus* and *Bacillus sp.*, but not against P. syringae, is a result similar to those previously reported in studies that compare the effect of a 2-alkyl-4-hydroxyquinoline (AHQ) against *S. aureus* and *P. aeruginosa*. Comparing our results with those

reported in the aforementioned studies, it highlights the fact that both AQM and AHQ contain a quinoline ring substituted in 2- and 4-position and both molecules were applied to cultures of *S. aureus* and *Pseudomonas*.[36] Although the biochemical explanation for the negative effect of AHQ on the growth of *S. aureus* is unknown, it has been suggested that its cell membrane is easily permeated by this molecule through passive diffusion, where it interferes with the electron transport chain, affecting cellular respiration, slowing cellular growth rate and inducing an extended Lag phase. On the other hand, these researchers argue that AHQ molecule is not able to penetrate *P. aeruginosa* due to the low permeability of its cell outer membrane and efficient elimination of antibiotics by means of efflux pumps,[37–39] and therefore this bacteria remained unaltered. Other researchers demonstrated that some AHQs molecules (as well as its N-oxide derivative) biosynthesized by *P. aeruginosa* act as anti-Staphylococcus agents, in similar way to commercial 4-quinolones, inhibiting genome replication by blocking topoisomerase enzyme activity.[36] Therefore, since AQM has a similar chemical structure and biological activity to the AHQs, it probably use the same mechanism of action described above for AHQ.

Table 1. The antibacterial activity (%) of AQM against pathogenic bacteria (n = 3; mean ± SD). The experimental time was established to be 20 h.

Molecule	Bacteria	Antibacterial Rate (%)				
		125 ppm	12.5 ppm	1.25 ppm	0.125 ppm	0.0125 ppm
AQM	*Bacillus sp.*	100.0 ± 0.7	36.3 ± 1.4	23.3± 2.0	20.2 ± 5.5	21.9 ± 3.4
AQM	*S. aureus*	99.7 ± 0.2	33.7 ± 5.6	29.0± 3.7	30.8 ± 2.9	32.7 ± 2.2
AQM	*Pcc*	51.7 ± 2.1	41.6 ± 0.4	10.1± 1.9	7.2 ± 0.5	9.3 ± 3.0
AQM	*R. solanacearum* [a]	17.3 ± 0.6	11.2 ± 1.0	9.9 ± 1.0	10.7 ± 0.7	10.5 ± 1.5
AQM	*P. syringae*	16.7 ± 3.7	6.3 ± 2.8	7.9 ± 4.8	11.8 ± 2.3	7.2 ± 3.0
AQM	*K. pneumoniae*	7.3 ± 0.7	4.6 ± 1.2	10.2± 1.6	10.1 ± 0.6	10.4 ± 0.8

[a] 18 h experiment

In addition to the presence of substituents at the 2- and 4-position of the quinoline ring of AQM, the chlorine atom at 7-position of the ring is a common structural feature among some antimicrobial quinoline derivatives,[13,14,27,40–42] which is essential in achieving antibacterial effect, according to de Souza et al.[43] With respect to the AHQs, or their 2-alkyl-4-quinolone tautomeric forms, it is important to highlight that they are biosynthesized and extracellularly released by *P. aeruginosa* during its colonization mechanism in the presence of other competing bacteria, with the aim of inhibiting the growth of these latter.

AHQs also act simultaneously as cell-to-cell signaling molecules that lead to the formation of biofilms, and along with other similar molecules, including 2-heptyl-3-hydroxy-4(1H)-quinolone (also known as the Pseudomonas Quinolone Signal, PQS), are part of the so-called "pseudanes". This name is derived from Pseudomonas, the bacterial genus in which such molecules were discovered, but they have also been found in bacteria of the genus *Burkholderia, Alteromonas* and *Pseudonocardia*.[37,44-46] Interestingly, like some "pseudanes" (e.g., PQS, AHQs), AQM is fluorescent and is quenched by interaction with ferric ion (Fe^{3+}),[47-49] as confirmed by fluorescence measurements performed in the present study (see Experimental Section). In addition, it is important to mention that: (1) ferric ion is one of the most important nutrients for bacteria, being essential for processes such as DNA replication, transcription, metabolism, and energy generation via respiration; and (2) the TSB medium used in the bioassays contains between 10 and 20 μM of Fe^{3+};[50] therefore the following question arises: ¿Is antibacterial activity of AQM related to its ability to interact with Fe^{3+} ions in the culture medium, and if so, is it works similar to some bacterial siderophores or competing siderophore? Although no additional experiments were performed in this study to attempt to answer this question, it is important to highlight that the bacteria most affected by AQM were the Gram-positive *S. aureus* and *Bacillus sp.*, while the Gram-negative bacteria remained unaffected (except *Pcc*, which is moderately affected). One possible explanation for the latter observation is that the Gram-positive bacteria exhibit relatively few iron-uptake mechanisms compared to Gram-negative bacteria (which are recognized by their diversity of highly efficient mechanisms of siderophore-mediated iron uptake);[51,52] this prevents Gram-positive bacteria from effectively competing for iron in the presence of other synthetic competing chelators, and according to our results most probably AQM is one competing iron-chelator (Figures 3 and 4). These results open the door to future studies to evaluate the potential effect of AQM on the iron uptake process in Gram-positive bacteria.

4. CONCLUSIONS

The following conclusions were drawn: (1) The compound AQM exhibited bacteriostatic effect on *S. aureus* and *Bacillus sp*., and was not active on the Gram-negative bacteria (*R. solanacearum, K. pneuminiae*, and *P. syringae*) except for Pcc whose growth rate decreased moderately (51.7%). (2) The fluorescence quenching of AQM by the addition of Fe^{3+} ion, suggests the formation of a non-fluorescent stable complex with Fe^{3+} ion, and consequently, this synthetic iron chelator (AQM) probably competed with the siderophores of both Gram-positive bacteria, leading to bacterial growth inhibition. These results show the potential use of AQM as new drug in antibacterial therapy or in the fluorometric detection of Fe^{3+} ions.

ACKNOWLEDGMENTS

REFERENCES

1. S. M. A. Hussaini, Expert Opin. Ther. Pat. **26**, 1201 (2016).
2. A. Marella, O. P. Tanwar, R. Saha, M. R. Ali, S. Srivastava, M. Akhter, M. Shaquiquzzaman, and M. M. Alam, Saudi Pharm. J. **21**, 1 (2013) .
3. C.-H. Lee and H.-S. Lee, J. Korean Soc. Appl. Biol. Chem. **52**, 331 (2009).
4. M. Artico, A. Mai, G. Sbardella, S. Massa, C. Musiu, S. Lostia, F. Demontis, and P. La Colla, Bioorganic Med. Chem. Lett. **9**, 1651 (1999).
5. G. S. Bisacchi, J. Med. Chem. **58**, 4874 (2015).
6. R. Cherdtrakulkiat, S. Boonpangrak, N. Sinthupoom, S. Prachayasittikul, S. Ruchirawat, and V. Prachayasittikul, Biochem. Biophys. Reports **6**, 135 (2016).
7. V. Prachayasittikul, V. Prachayasittikul, S. Prachayasittikul, and S. Ruchirawat, Drug Des. Devel. Ther. **7**, 1157 (2013).
8. M. Asif, Ann Med Chem Res **1**, 1003 (2014).
9. M. A. Kohanski, D. J. Dwyer, and J. J. Collins, Nat. Rev. Microbiol. **8**, 423 (2010).
10. V. Uivarosi, Molecules **18**, 11153 (2013).
11. C. Pelletier, P. Prognon, and P. Bourlioux, Antimicrob. Agents Chemother. **39**, 707 (1995).
12. H. Huber-Emden, A. Hubele, and G. Klahre, Patent US3873703A, 1975.
13. D. Ghisalberti, A. Mahamoud, J. Chevalier, M. Baitiche, M. Martino, J.-M. Pagès, and J. Barbe, Int. J. Antimicrob. Agents **27**, 565 (2006).
14. J.-M. Rolain, P. Colson, and D. Raoult, Int. J. Antimicrob. Agents **30**, 297 (2007).
15. A. So, B. A. Nacev, C. R. Chong, H. C. Bhang, J. Xu, J. S. Shim, J. O. Liu, K. C. Han, M. G. Pomper, S. Bhat, S. Dhara, and Y. Matsui, JNCI J. Natl. Cancer Inst. **102**, 1855 (2010).
16. B. Mirković, B. Markelc, M. Butinar, A. Mitrović, I. Sosič, S. Gobec, O. Vasiljeva, B. Turk, M. Čemažar, G. Serša, and J. Kos, Oncotarget **6**, 19027 (2015).
17. J. Lazovic, L. Guo, J. Nakashima, L. Mirsadraei, W. Yong, H. J. Kim, B. Ellingson, H. Wu, and W. B. Pope, Neuro. Oncol. **17**, 53 (2014).
18. W.-L. Chang, L.-C. Hsu, W.-J. Leu, C.-S. Chen, and J.-H. Guh, Oncotarget **6**, 39806 (2015).
19. V. Prachayasittikul, W. Chan-On, H. Nguyen Thi Bich, N. Songtawee, W. Suwanjang, and S. Prachayasittikul, Drug Des. Devel. Ther. **9**, 2033 (2015).
20. H. Jiang, J. E. Taggart, X. Zhang, D. M. Benbrook, S. E. Lind, and W.-Q. Ding, Cancer Lett. **312**, 11 (2011).
21. P. Huang and Q. Li, Patent WO 2017/173278 A1, 2017.
22. M. Fiorillo, R. Lamb, H. B. Tanowitz, A. R. Cappello, U. E. Martinez-Outschoorn, F. Sotgia, and M. P. Lisanti, Aging (Albany. NY). **8**, 1593 (2016).
23. P. Pantziarka, V. Sukhatme, L. Meheus, V. Sukhatme, and G. Bouche, BioRxiv 197434 (2017).
24. Q. Dong, J. Luo, W. Qiu, L. Cai, S. Anjum, B. Li, M. Hou, G. Xie, G. Sun, Q. Dong, J. Luo, W. Qiu, L. Cai, S. I. Anjum, B. Li, M. Hou, G. Xie, and G. Sun, Molecules **21**, 978 (2016).
25. H. Valle, R. Palao-Suay, M. R. Aguilar, J. S. Román, J. Becerra, B. Rivas, and R. V. Mangalaraja, J. Appl. Polym. Sci. **136**, 47545 (2019).
26. CLSI, Methods for Dilution Antimicrobial Susceptibility Tests for Bacteria That Grow Aerobically (CLSI Document M07-A9), Approved Standard – 9th Ed. (Clinical and Laboratory Standards Institute, Wayne, Pennsylvania, 2012), pp. 16–20.
27. S. Singh, K. K. Roy, S. R. Khan, V. K. Kashyap, A. Sharma, S. Jaiswal, S. K. Sharma, M. Y. Krishnan, V. Chaturvedi, J. Lal, S. Sinha, A. Dasgupta, R. Srivastava, and A. K. Saxena, Bioorg. Med. Chem. **23**, 742 (2015).
28. I. J. Pachter, J. Am. Chem. Soc. **75**, 3026 (1953).
29. A. Esparza-Ruiz, C. Herrmann, J. Chen, B. O. Patrick, E. Polishchuk, and C. Orvig, Inorganica Chim. Acta **393**, 276 (2012).
30. *B. Valeur and M. N. Berberan-Santos, Molecular Fluorescence : Principles and Applications, 2nd Ed. (Wiley-VCH, Weinheim, 2012), pp. 72–74.
31. D. S. Karpovich and G. J. Blanchard, J. Phys. Chem. **99**, 3951 (1995).
32. Y. W. Choi, G. J. Park, Y. J. Na, H. Y. Jo, S. A. Lee, G. R. You, and C. Kim, Sensors Actuators B Chem. **194**, 343 (2014).
33. X. Bao, X. Cao, X. Nie, Y. Xu, W. Guo, B. Zhou, L. Zhang, H. Liao, and T. Pang, Sensors Actuators B Chem. **208**, 54 (2015).
34. P. Kaur, H. Kaur, and K. Singh, RSC Adv. **3**, 64 (2013).
35. X. Yang, P. Zhao, J. Qu, and R. Liu, Luminescence **30**, 592 (2015).
36. Z. A. Machan, G. W. Taylor, T. L. Pitt, P. J. Cole, and R. Wilson, J. Antimicrob. Chemother. **30**, 615 (1992).
37. F. Salvaggio, J. T. Hodgkinson, L. Carro, S. M. Geddis, W. R. J. D. Galloway, M. Welch, and D. R. Spring, European J. Org. Chem. 434 (2016).
38. P. A. Lambert, J. R. Soc. Med. **95 Suppl 4**, 22 (2002).
39. J. Ruiz, J. Antimicrob. Chemother. **51**, 1109 (2003).
40. R. Clinton and C. Suter, Patent US2505462A, 1950.
41. M. Rudrapal and D. Chetia, Int. J. ChemTech Res. **2**, 1606 (2010).
42. R. Jagadeesh, K. N. Saivisveswar, and S. P. Revankar, Sch. J. App. Med. Sci. **2**, 3046 (2014).
43. M. V. N. de Souza, K. C. Pais, C. R. Kaiser, M. A. Peralta, M. de L. Ferreira, and M. C. S. Lourenço, Bioorg. Med. Chem. **17**, 1474 (2009).
44. M. Toyofuku, T. Nakajima-Kambe, H. Uchiyama, and N. Nomura, Microbes Environ. **25**, 1 (2010).
45. S. Heeb, M. P. Fletcher, S. R. Chhabra, S. P. Diggle, P. Williams, and M. Cámara, FEMS Microbiol. Rev. **35**, 247 (2011).
46. H. Budzikiewicz, Siderophores of the Pseudomonadaceae sensu stricto (Fluorescent and Non-Fluorescent Pseudomonas spp.), in Progress in the Chemistry of Organic Natural Products, ed. by W. Herz, H. Falk, and G. W. Kirby (Springer Vienna, Vienna, 2004), p. 81.
47. S. P. Diggle, S. Matthijs, V. J. Wright, M. P. Fletcher, S. R. Chhabra, I. L. Lamont, X. Kong, R. C. Hider, P. Cornelis, M. Cámara, and P. Williams, Chem. Biol. **14**, 87 (2007).
48. P. W. Royt, R. V. Honeychuck, V. Ravich, P. Ponnaluri, L. K. Pannell, J. S. Buyer, V. Chandhoke, W. M. Stalick, L. C. DeSesso, S. Donohue, R. Ghei, J. D. Relyea, and R. Ruiz, Bioorg. Chem. **29**, 387 (2001).
49. G. Palmer, J. Schertzer, L. Mashburn-Warren, M. Whiteley, Methods Mol. Biol. **692**, 207 (2011).
50. W. Raza, W. Hongsheng, and S. Qirong, Brazilian Arch. Biol. Technol. **53**, 1145 (2010).
51. F. Imperi, K. A. Mettrick, M. Shirley, F. Tiburzi, R. C. Draper, P. Visca, and I. L. Lamont, Iron Transport and Signaling in Pseudomonads, in Pseudomonas, ed. by B. H. Rehm (Wiley-VCH Verlag GmbH & Co. KGaA, Weinheim, Germany, 2008), p. 129.
52. J. S. Brown and D. W. Holden, Microbes Infect. **4**, 1149 (2002).